Symbolic-Numerical Algorithm for Solving the Problem of Heavy Ion Collisions in an Optical Model with a Complex Potential

A. A. Gusev[1,2(✉)], O. Chuluunbaatar[1,3], V.L. Derbov[4], R.G. Nazmitdinov[1,2], S.I. Vinitsky[1,5], P.W. Wen[6], C.J. Lin[6,7], H.M. Jia[6], and L.L. Hai[8]

[1] Joint Institute for Nuclear Research, 141980 Dubna, Russia
gooseff@jinr.ru
[2] Dubna State University, 141982 Dubna, Russia
[3] Institute of Mathematics and Digital Technology, Mongolian Academy of Sciences, 13330 Ulaanbaatar, Mongolia
[4] Chernyshevsky Saratov National Research State University, Saratov, Russia
[5] Peoples' Friendship University of Russia (RUDN University), 117198 Moscow, Russia
[6] China Institute of Atomic Energy, 102413 Beijing, China
[7] College of Physics and Technology & Guangxi Key Laboratory of Nuclear Physics and Technology, Guangxi Normal University, 541004 Guilin, China
[8] Ho Chi Minh City University of Education, Ho Chi Minh City, Vietnam

Abstract. We present an original algorithm in the MAPLE system for solving the scattering problem in single-channel approximation of the coupled-channel method of the optical model (OM) described by a second-order ordinary differential equation (ODE) with a complex-valued potential and regular boundary conditions. The complex-valued potential consists of the known real part, which is a sum of the nuclear potential, the Coulomb potential, and the centrifugal potential, and the imaginary part, which is a product of the unknown coupling constant $g(E)$, depending on the collision energy E of a pair of ions, and the derivative of the real part of the known nuclear potential with respect to the ODE independent variable.

The presented algorithm implements the solution of the inverse problem, i.e., calculates the unknown coupling constant $g(E)$ and scattering matrix $S(g(E), E)$ from condition $|S(g(E), E)|^2 = 1 - |T(E)|^2$ by means of the secant method. The required amplitudes of transmission $T(E)$ and reflection $R(E)$ subject also to the condition $|R(E)|^2 = 1 - |T(E)|^2$ of the model with incoming wave boundary conditions (IWBCs) are previously calculated by the standard MAPLE implemented KANTBP 4M program.

The algorithm provides a one-to-one correspondence between the OM with a complex-valued potential and the model of IWBCs with a real-valued potential.

F. Boulier et al. (Eds.): CASC 2023, LNCS 14139, pp. 128–140, 2023.
https://doi.org/10.1007/978-3-031-41724-5_7

The efficiency of the proposed approach is shown by solving numerically the scattering problem and calculating the reference fusion cross section for a pair of heavy ions $^{16}O+^{144}Sm$ in the single-channel approximation of the close-coupling method.

Keywords: Symbolic-numerical algorithm · Optical model with complex-valued potential · Incoming wave boundary conditions model · Heavy ion collision problem

1 Introduction

In the coupled-channel (CC) method for describing sub-barrier reactions with heavy ions, the scattering problem is solved for a system of second-order ordinary differential equations (ODEs) with complex-valued optical model (OM) potentials and the ODE solutions subjected to regular boundary conditions (BCs). This approach has started from [1–3] and was continued in [4–6].

The alternative incoming wave boundary condition (IWBC) model uses real-valued potentials, each of them being a sum of a short-range nuclear potential of interaction between two heavy particles, a long-range real Coulomb potential, and a long-range real centrifugal potential [7–13]. In the IWBC model, to formulate correctly the Robin BCs with the correct set of threshold energies in the coupled channel method, it was required to diagonalize the coupling matrix of the effective potentials of coupled channels at the potential minimum point inside the potential barrier [14–16]. Such a formulation of the IWBCs with diagonalization of the potential channel coupling matrix at the minimum point inside the potential barrier was reported in recent papers [17,18] and implemented in the KANTBP 3.0, KANTBP 3.1 programs [19,20].

This circumstance allowed us to return to considering the OM with the complex-valued potential [2]. For simplicity, it is specified by the real-valued spherical Wood–Saxon nuclear potential and the imaginary part of the surface nuclear potential of the OM given as a product of the unknown coupling constant and derivative of the known nuclear potential with respect to the ODE independent variable, which is sufficient for low collision energies [21].

In the OM with a complex-valued potential, one of the main problems is to find the coupling constant parameter, which depends on the collision energy of two heavy ions. The problem of including the imaginary part into the nuclear potential is traditionally solved by fitting the coupling constant value to the experimental data on the cross section of the reaction, which depends on the collision energy of the pair of heavy ions.

To specify the real part of the nuclear potential, it is sufficient to use the well-known tabulated parameters of the Wood–Saxon nuclear potential and its multipole deformation in the collective nuclear model [22], which correspond to the experimental data on the reaction cross sections depending on the collision energy [23]. Thus, to calculate the coupling constants for the imaginary part of the nuclear potential in OMs, it is sufficient to construct an algorithm that uses

as the initial data the transmission and reflection coefficients of the IWBC model previously calculated by the KANTBP 4M program [24] implementing the finite element method in MAPLE [25].

This paper presents an original algorithm implemented in the MAPLE system for calculating the parameter $g(E) > 0$, the coupling constant of the imaginary part of the complex-valued potential depending on the collision energy E of a pair of ions, in the OM of the scattering problem described by the second-order ODEs with complex-valued potential using the KANTBP 4M program.

In OM, the coupling constant $g(E) > 0$ is calculated from the condition

$$1 - |S_L(g(E), E)|^2 = |T_L(E)|^2,$$

where $S_L(g(E), E)$ is the scattering matrix depending on $g(E)$ and E, and $T_L(E)$ is the transmission amplitude depending only on E of the IWBC model with the real-valued potential. The scattering matrix $S_L(g(E), E)$ is determined by solving the ODE subject to regular BCs of a scattering problem for the OM with complex-valued potential with given $g(E)$. The transmission amplitude $T_L(E) = T_L^{\mathrm{IWBC}}(E)$ is extracted from the solution of the ODE subject to IWBC. Thus, the proposed algorithm provides a one-to-one correspondence between the OM with a complex-valued potential and the IWBC model with a real-valued potential announced in the pioneer paper [1].

The efficiency of the proposed algorithm is shown by solving the scattering problem and calculating the reference fusion cross section of a pair of heavy ions ^{16}O+^{144}Sm in the single-channel approximation of the coupled-channel method with the complex-valued potential.

The paper is organized as follows. In Sect. 2, we formulate the OM in the single-channel approximation. Section 3 presents the OM algorithm. Section 4 presents a numerical example, in which the solutions of the scattering problem and the reference cross section for the fusion of a pair of heavy ions ^{16}O+^{144}Sm and the coupling constant of the imaginary part of the surface nuclear potential are calculated. In Conclusion, the main results are summarized and further prospects for applying the proposed approach are outlined.

2 Optical Model and IWBC Model in the Single-Channel Approximation

First, we compare the single-channel approximation of the OM [2] and the IWBC model [10,20] without nuclear deformation coupling described by the equation

$$\left(-\frac{\hbar^2}{2\mu}\triangle_{\mathbf{r}} + V(g, \mathbf{r}) - E\right)\Psi(\mathbf{r}) = 0, \tag{1}$$

where $\Psi(\mathbf{r}) = r^{-1}\sum_{Lm}\Psi_L(r)Y_L^m(\theta, \varphi)$, $Y_L^m(\theta, \varphi)$ is a spherical harmonic [21], and $\Psi_L(r)$ satisfies the radial equation

$$\left(-\frac{\hbar^2}{2\mu}\frac{d^2}{dr^2} + V_L(g, r) - E\right)\Psi_L(r) = 0. \tag{2}$$

In the OM and IWBC model, the radial wave function $\Psi_L(r)$ is subjected to different BCs in the boundary points of different intervals $r \in [r_L^{\min}, r_L^{\max}]$ presented in Sect. 3.

For the OM in Eq. (2), $V_L(g,r)$ is the complex-valued potential given by a sum of four terms:

$$\begin{aligned} V_L(g,r) &= V(g,\mathbf{r}) + \frac{\hbar^2}{2\mu}\frac{L(L+1)}{r^2} \\ &= V_N(r) - \imath g(E)\frac{dV_N(r)}{dr} + \bar{V}_C(r) + \frac{\hbar^2}{2\mu}\frac{L(L+1)}{r^2}, \end{aligned} \tag{3}$$

namely, the real-valued nuclear Woods–Saxon potential

$$V_N(r) = -\frac{V_0}{1+\exp((r-R_0)/a)}, \tag{4}$$

the imaginary part of the surface nuclear potential including the unknown real-valued coupling constant $g(E)$ depending on collision energy E

$$-\imath g(E)\frac{dV_N(r)}{dr}, \tag{5}$$

the Coulomb potential [26] describing the interaction of the projectile charge Z_P with the target charge Z_T, uniformly distributed over a ball of radius R_C depending on the masses of the projectile A_P and the target A_T, and parameter R_{00}

$$\begin{aligned} \bar{V}_C(r) &= Z_P Z_T \begin{cases} 1/r, & r \geq R_C, \\ (3R_C^2 - r^2)/(2R_C^3), & r < R_C, \end{cases} \\ R_C &= R_0 = R_{00}(A_P^{1/3} + A_T^{1/3}). \end{aligned} \tag{6}$$

The last term in Eq. (3) is a rotation centrifugal potential.

For solving a scattering problem in the IWBC model in Eq. (2), the complex-valued potential $V_L(g,r)$ is replaced to the real-valued potential $V_L(r)$ determined by the following:

$$V_L(r) = V_L\Big(g=0, \max\left(r, r_L^{\min}\right)\Big), \tag{7}$$

where the value of $r_L^{\min}$ depends on the angular momentum L and is determined by the condition

$$E > V_L^{\min} = V_L\Big(g=0, r_L^{\min}\Big), \quad \left.\frac{dV_L^{\min}(g=0,r)}{dr}\right|_{r=r_L^{\min}} = 0. \tag{8}$$

The value of $L_{\max}$ is restricted by the limited value of the incident energy E in the entrance channel: $E = V_L(r_L^{\min})$, where $V_L(r_L^{\min})$ is the potential minimum, $L = 0, \ldots, L_{\max}$.

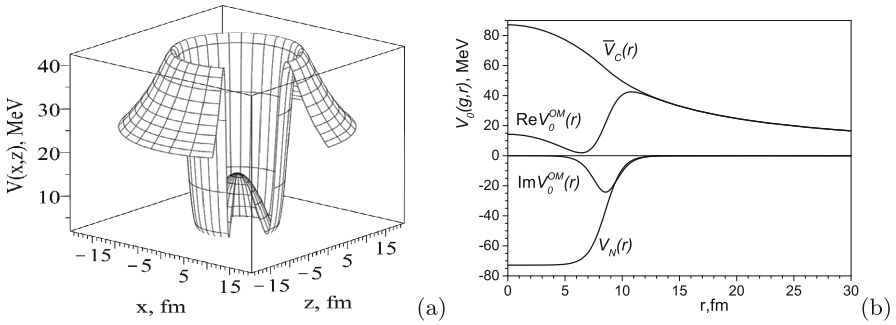

Fig. 1. OM potential $V(x,z) = \Re V(g,\mathbf{r})$ in the xz-plane (a) and $V_L(g,r)$ and its components at $g = 1$ and $L = 0$ (b) for a pair of heavy ions ^{16}O+^{144}Sm

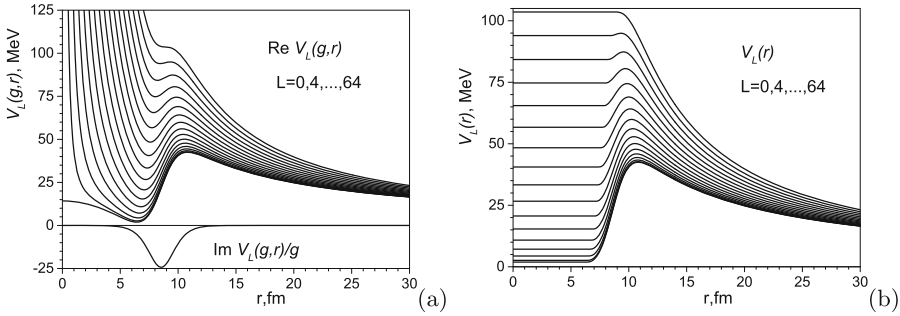

Fig. 2. Real and imaginary parts of the potentials $V_L(g,r)$ of OM (a) and the real-valued potential $V_L(r)$ of IWBC model (b) for a pair of heavy ions ^{16}O+^{144}Sm

In the IWBC model, the nuclear potential $V_N(r)$ having a constant value of $V_N(r = r_L^{\min})$ for $r \le r_L^{\min}$, the value of $r_L^{\min}$ is determined by the condition (8).

In Fig. 1 (a), we show the real part $\Re V(g,\mathbf{r})$ of the OM potential in the xz-plane. Figure 1 (b) shows the components of the potential $V_L(g,r)$ at $L = 0$ and $g = 1$. The real and imaginary parts of the potentials $V_L(g,r)$ and $V_L(r)$ for ^{16}O+^{144}Sm are shown in Fig. 2 (a) for the OM model and in Fig. 2 (b) for the IWBC model, respectively.

The parameters of the problem for the ^{16}O+^{144}Sm reaction are:

$$A_P = 16, \quad A_T = 144.0, \quad Z_P = 8, \quad Z_T = 62, \quad \mu = A_P A_T/(A_P + A_T);$$
$$V_0 = 105 \text{ MeV}, \quad R_{00} = 1.1 \text{ fm}, \quad A_0 = 0.75 \text{ fm};$$
$$R_0 = R_{00}(A_P^{1/3} + A_T^{1/3}) \quad \text{in the zeroth approximation.}$$

3 The Optical Model Algorithm

The following algorithm calculates the unknown coupling constant $g(E) > 0$ for a given value of energy E from the condition

$$1 - |S_L(g(E),E)|^2 = |T_L(E)|^2.$$

The transmission $T_L(E)$ amplitude and the reflection $R_L(E)$ amplitude and the eigenfunction $\Psi_L(r)$ are calculated in advance by numerically solving the ODE (2) with the real-valued potential $V_L(r)$ from (7) subject to IWBCs for a given value of energy E. The scattering matrix $S_L(g(E), E)$ and eigenfunction $\Psi_L(r)$ are calculated by numerically solving the ODE (2) subject to regular BCs of a scattering problem for the OM with complex-valued potential $V_L(g(E), r)$ from (3) with given $g(E)$.

Algorithm OMCCG.

Input $E \in \{E_1, \ldots, E_n\}$ is a grid of real values of collision energies E.

Step 1. Finding the parameter $g(E) > 0$ on the grid $E \in \{E_1, \ldots, E_n\}$ by the secant method with a given tolerance $0 < \epsilon \ll 1 \simeq (10^{-8}, 10^{-13})$.

Step 1.1. We put $g = 0$ and calculate $G_0 = -|T_L(E_i)|^2$ using **Algorithm IWBCM.**

Step 1.2. We choose the initial values of $g_0 = \{0, i = 1, 2; g(E_{i-2}), i = 3, 4, \ldots, n\}$, $g_1 = \{10^{-4}, i = 1; g(E_{i-1}), i = 2, 3, \ldots, n\}$, and calculate

$$G_1 = 1 - |S_L(g_1, E_i)|^2 - |T_L(E_i)|^2,$$

where $S_L(g_1, E_i)$ is computed using the **OM algorithm** and the value of $|T_L(E_i)|^2$ is calculated at *Step 1.1.*

Step 1.3. For $k = 1, 2, \ldots$ while $|g_k - g_{k-1}| > \epsilon$: we put

$$g_{k+1} = g_k - G_k \frac{g_k - g_{k-1}}{G_k - G_{k-1}},$$

and calculate

$$G_{k+1} = 1 - |S_L(g_{k+1}, E_i)|^2 - |T_L(E_i)|^2.$$

Step 1.4. The fusion cross section $\sigma_{\text{fus}}(E)$ is calculated using the formula

$$\sigma_{\text{fus}}(E) = \sum_{L=0} \sigma_{\text{fus}}^L(E), \quad \sigma_{\text{fus}}^L(E) = \frac{\pi}{k^2}(2L+1)(1 - |S_L(g, E)|^2). \quad (9)$$

Output. Sets $g(E)$, $\Psi_L(r)$, $S_L(g, E)$, and $\sigma_{\text{fus}}^L(E)$ of scattering states at the given real energy E: on the grid $E \in \{E_1, \ldots, E_n\}$ in the OM.

End of Algorithm OMCCG

Algorithm IWBCM.

Input $r = [r_L^{\min}, r_L^{\max}]$ is the interval of independent variable of ODE of the IWBC model; E is the collision energy; $V_L(r)$ is the real-valued potential from (7).
Solving the scattering problem for Eq. (2) of the IWBC model with the real-valued potential $V_L(r)$ from (7) and Robin BC at the boundary points of the interval $r = [r_L^{\min}, r_L^{\max}]$,

$$\frac{d\Psi_L(r)}{dr} = \mathcal{R}(r)\Psi_L(r), \quad \mathcal{R}(r) = \frac{d\Psi_L^{\rm as}(r)}{dr}\frac{1}{\Psi_L^{\rm as}(r)} \tag{10}$$

which follows from the asymptotic solution [20]

$$\Psi_L^{\rm as}(r_L^{\rm min}) = \frac{\exp(-\imath K r)}{\sqrt{K}} T_L^{\rm IWBC}(E),\ K = \sqrt{\frac{2\mu}{\hbar^2}}\sqrt{E - V_L(r_L^{\rm min})}, \tag{11}$$

$$\Psi_L^{\rm as}(r_L^{\rm max}) = \frac{1}{\sqrt{k}}(\hat{H}_L^-(kr) - \hat{H}_L^+(kr) R_L^{\rm IWBC}(E)), \quad k = \sqrt{\frac{2\mu}{\hbar^2}}\sqrt{E}.$$

Here $\hat{H}_L^{\pm}(kr)$ are the normalized outgoing and incoming Coulomb partial wave functions,

$$\hat{H}_L^{\pm}(kr) = [\pm\imath F_L(\eta, kr) + G_L(\eta, kr)]\exp(\mp\imath\delta_L^C) \tag{12}$$

and $F_L(\eta, kr)$ and $G_L(\eta, kr)$ are the regular and irregular Coulomb partial wave functions, $\eta = kZ_P Z_T e^2/(2E)$ is the Sommerfeld parameter, $\delta_L^C = \arg\Gamma(L + 1 + \imath\eta)$ is the Coulomb phase shift [27,28].
Calculating $\Psi_L(r)$, $T_L(E) \equiv T_L^{\rm IWBC}(E)$ and $R_L(E) \equiv R_L^{\rm IWBC}(E)$, testified to the following condition:

$$|T_L(E)|^2 + |R_L(E)|^2 = 1.$$

Output. $\Psi_L(r)$ and $T_L(E)$, and $R_L(E)$ of scattering states at the given real energy E in the IWBC model.

End of Algorithm IWBCM

Algorithm OM

Input. KeyOM = 0 is computing scattering states; KeyOM = 1 is computing metastable states;
$r = [r_L^0, r_L^{\rm max}]$ is the interval of the independent variable of ODE (2) of the IWBC model; E is the collision energy; $g(E)$ is the given coupling constant depending on E; $V_L(g(E), r)$ is the real-valued potential from (3).
If KeyOM = 0 then go to 1 else go to 2 fi.

1. Solving the scattering problem for Eq. (2) with respect to $\Psi(r)$ and $S_L(g, E)$ of the OM with the complex-valued potential $V_L(g, r)$ (3) for a given value of $g(E)$ calculated at *Step 1.3* of **OMCCG** algorithm and mixed BCs at the boundary points of interval $r \in [r_L^0, r_L^{\rm max}]$:
the Neumann BC at $r = r_L^0$,

$$\left.\frac{d\Psi_L^{\rm as}(r)}{dr}\right|_{r=r_L^0} = 0, \quad r_L^0 \le r_L^{\rm min},$$

and the Robin BC at $r = r_L^{\rm max}$,

$$\frac{d\Psi_L(r)}{dr} = \mathcal{R}(r)\Psi_L(r), \quad \mathcal{R}(r) = \frac{d\Psi_L^{\rm as}(r)}{dr}\frac{1}{\Psi_L^{\rm as}(r)}$$

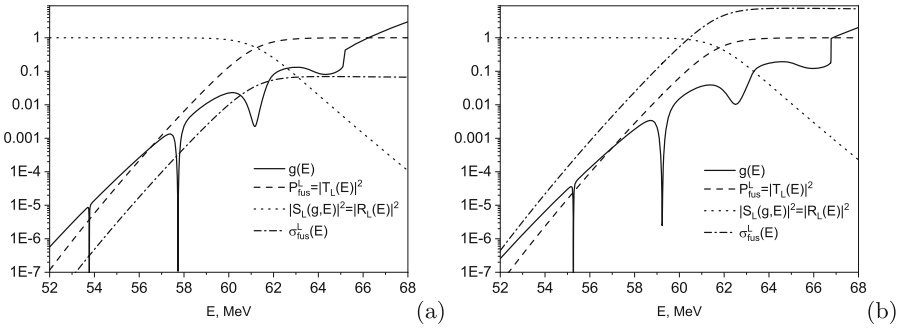

Fig. 3. Collision energy dependence of the parameter $g(E)$, the fusion probability $P^L_{\rm fus} = |T_L(E)|^2$, the reflection (scattering) coefficient $|R_L(E)|^2 = |S_L(g(E), E)|^2$, as well as the smooth fusion partial cross section $\sigma^L_{\rm fus}(E)$ (in mb) of sub-barrier fusion reaction for a pair of heavy ions ^{16}O+^{144}Sm for $L = 0$ (a) and $L = 5$ (b)

which follows from the asymptotic solution [20]

$$\Psi^{\rm as}_L(r^{\max}_L) = \frac{\hat{H}^-_L(kr) - \hat{H}^+_L(kr)S_L(g,E)}{\sqrt{k}}.$$

2. Calculating the eigenfunctions $\Psi_{L\nu}(r)$ and the complex-valued eigenenergies $E^M_{L,\nu}$ of metastable states at a given value $g(E) > 0$ calculated at *Step 1.3* of **OMCCG** algorithm with the outgoing wave at the boundary point $r = r^{\max}_L$ [29],

$$\Psi^{\rm as}_{L\nu}(r^{\max}_L) = \frac{1}{\sqrt{k}}\hat{H}^+_L(kr)O^{\rm OM}_L(E^M_{L,\nu}), \quad k = \sqrt{\frac{2\mu}{\hbar^2}}\sqrt{E^M_{L,\nu}},$$

where $O^{\rm OM}_L(E^M_{L,\nu})$ is the amplitude of outgoing wave.

Output. $\Psi_L(r)$ and $S_L(g, E)$ of scattering states at the given real energy E in the OM or eigenfunctions $\Psi_{L\nu}(r)$ and complex eigenenergies $E^M_{L,\nu}$ of metastable states in the OM.

End of Algorithm OM

Remark. Instead of the Neumann BC, one can use also the Robin BC $r = r^0_L$, which follows from the regular asymptotic solution

$$\Psi^{\rm as}_L(r^0_L) = \frac{r^{L+1}\exp(-\imath Kr)}{\sqrt{K}}A^{OM}_L(E), \quad K = \sqrt{\frac{2\mu}{\hbar^2}}\sqrt{E - V_L(r^0_L)},$$

where $A^{OM}_L(E)$ is a normalization factor.

4 Benchmark Calculations

An example of sub-barrier fusion reaction for a pair of heavy ions ^{16}O+^{144}Sm is numerically studied using the IWBC model and the OM. To solve the scattering problem and to calculate the metastable states, we use the KANTBP 4M program [24] implementing the finite element method in MAPLE [25].

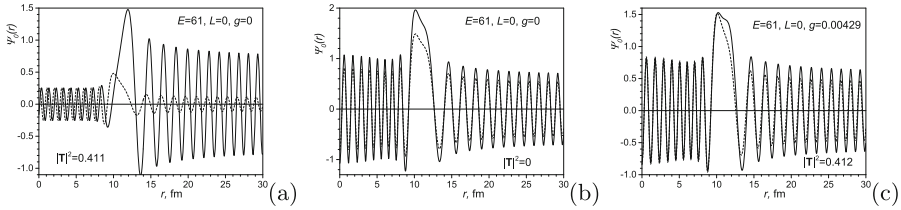

Fig. 4. Eigenfunctions $\Psi_0(r) = \Psi_L(r)$ of scattering states of sub-barrier fusion reaction for a pair of heavy ions ^{16}O+^{144}Sm at a non resonance energy of $E = 61$ MeV, $L = 0$. IWBC (a) in comparison with OM at $g = 0$ (b) and $g = 0.00429$ (c)

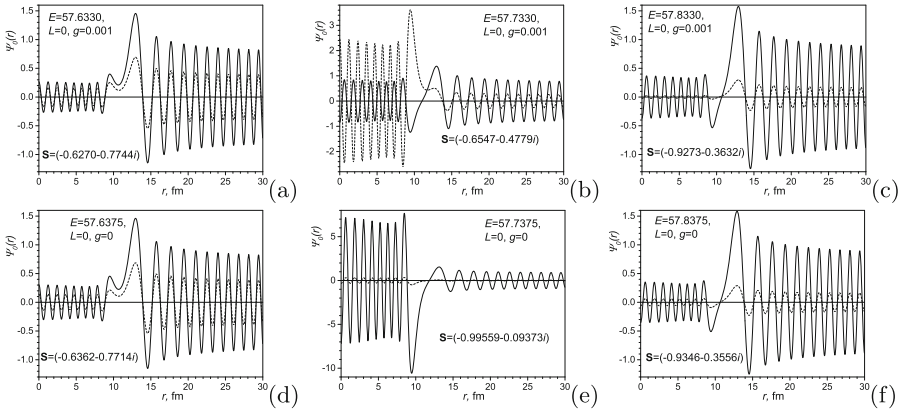

Fig. 5. Eigenfunctions $\Psi_0(r) = \Psi_L(r)$ of the OM scattering states of sub-barrier fusion reaction for a pair of heavy ions ^{16}O+^{144}Sm at $L = 0$ in the vicinity of resonance (the second peak of $g(E)$ in Fig. 3), $E = E^{\rm res} \approx 57.7330$ MeV at $g = 0.001$ (b) and $E = E^{\rm res} \approx 57.7375$ MeV at $g = 0$ (e), in comparison with the eigenfunctions of scattering states at $E = E^{\rm res} \pm 0.1$ MeV (a,c,d,f)

Figure 3 illustrates the collision energy dependence of the parameter $g(E)$, the fusion probability $P^L_{\rm fus} = |T_L(E)|^2$, the reflection (scattering) coefficient $|R_L(E)|^2 = |S_L(g(E), E)|^2$, as well as the smooth fusion partial cross section $\sigma^L_{\rm fus}(E)$ (in mb) at $L = 0$ (a) and $L = 5$ (b). The resonance structure of the coupling constant $g(E)$ is seen, which testifies for the existence of metastable states, manifesting themselves as resonances in the elastic scattering in the interval of energies $E \in [52, 68]$ MeV.

Figure 4 (a) shows the eigenfunctions of the IWBC scattering states for comparison with OM ones at $g = 0$ (Fig. 4 (b)) and at $g = 0.00429$ (Fig. 4 (c)) for a non-resonance energy of $E = 61$ MeV. At first glance, these functions have similar behavior, but the real part of the IWBC function has $v = 18$ nodes in the interval $r \in [0, 10]$ and the transmission coefficient equal to $|T_0|^2 = 0.411$ that corresponds to a partial transmission, whereas the OM function has $v = 17$ nodes in the interval $r \in [0, 10]$ and the transmission coefficient equal to $|T_0|^2 = 0$, i.e., $|R_0|^2 = 1$, which corresponds to a total reflection.

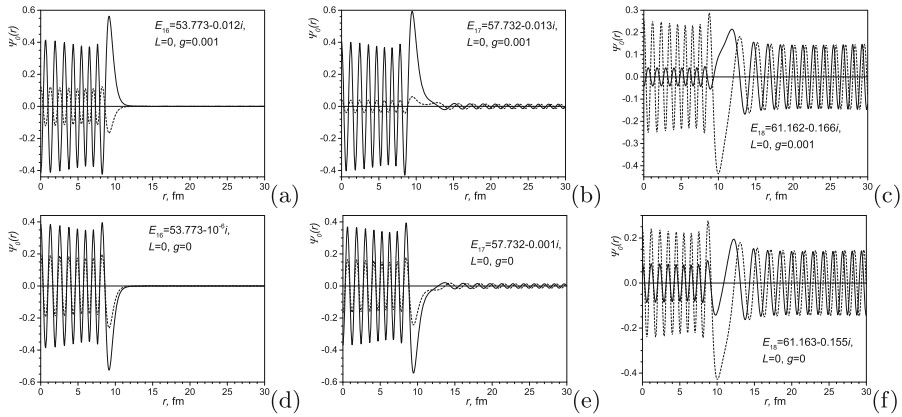

Fig. 6. Eigenfunctions $\Psi_0(r) = \Psi_{L\nu}(r)$ of the three metastable states at $L = 0$ and $\nu = 16, 17, 18$ with complex energies $E_{L,\nu} = E_\nu$: $E_{16} = 53.773 - 0.012\imath$ (a), $E_{17} = 57.732 - 0.013\imath$ (b) and $E_{18} = 61.162 - 0.166\imath$ (c) at $g = 0.001$ in the vicinity of the first, second, and third peaks of $g(E)$, in comparison with three metastable states $E_{16} = 53.773 - 10^{-6}\imath$ (d), $E_{17} = 57.732 - 0.001\imath$ (e) and $E_{18} = 61.163 - 0.155\imath$ (f) at $g = 0$ for a pair of heavy ions $^{16}\mathrm{O}+^{144}\mathrm{Sm}$

Note that the IWBC function is calculated in the interval $r \in [r_L^{\min}, r_L^{\max}]$ with Robin BCs. Here we continue this function over the interval $r \in (0, r_L^{\min}]$ using its asymptotic behavior (10). The latter is known because the nuclear potential $V_N(r) = V_N(r_L^{\min})$ in this interval, as shown by horizontal lines in Fig. 2 (b). However, in all papers exploiting the IWBC model, the behavior of wave functions in this interval is not discussed. This is because of the difference in the definition of potentials and BCs in these two models. Indeed, the OM potential is prolonged till the vicinity $r_L^0 \ll r_L^{\min}$ and the regular Neumann BC are used at r_L^0, while in the IWBC model, the potential is cut off at $r = r_L^{\min}$ and the Robin BC is used at this point. To compensate for this principal difference, the imaginary part of the optical potential is switched on with the help of the initially unknown coupling constant $g(E) > 0$. The corresponding scattering state eigenfunction of OM at $g = 0.00429$ has the same $\upsilon = 17$ nodes in the interval $r \in [0, 10]$ and yields the transmission coefficient $|T_0|^2 = 0.412$, as shown in Fig. 4 (c).

This observation gave us an opportunity to propose the above algorithm, in which the agreement of OM and IWBC wave functions at $L = 0$ is achieved by solving an inverse problem, namely, by calculating the unknown coupling constant $g(E)$ from the reflection $R_0(E)$ and transmission $T_0(E)$ amplitudes, determined in advance together with the required wave functions of the IWBC model.

The resonance peaks of $g(E)$ correspond to the appearance of metastable states with complex energy $E_{L,\nu}^M$ at $\Im E_{L,\nu}^M < 0$, such that the real part of a metastable state energy is close to the resonance scattering energy $E^{\mathrm{res}} \approx \Re E_{L,\nu}^M$. The eigenfunctions of scattering states with the resonance energy $E^{\mathrm{res}} \approx 57.73$ at $g = 0.001$ and $g = 0$ in the vicinity of the second peak of $g(E)$ are shown

Table 1. The complex energy $E^M_{L,\nu} = \Re E^M_{L,\nu} + \imath \Im E^M_{L,\nu}$ of metastable states and the corresponding shape resonance energies $E^{\rm res} \approx \Re E^M_{L,\nu}$ of scattering problem OM at $L = 0$, $g = 0$ and $g = g_{\rm res}$ for a pair of heavy ions ^{16}O+^{144}Sm

ν	$E^M_{L,\nu}(g = 0)$	$E^{\rm res}(g = 0)$	$g = g_{\rm res}$	$E^M_{L,\nu}(g = g_{\rm res})$	$E^{\rm res}(g = g_{\rm res})$
16	$53.7731 - 10^{-6}\imath$	53.7729	$5 \cdot 10^{-13}$	$53.7731 - 1.2 \cdot 10^{-6}\imath$	53.7731
17	$57.7328 - 0.0012\imath$	57.7326	$1 \cdot 10^{-7}$	$57.7328 - 0.0012\imath$	57.7329
18	$61.1639 - 0.1558\imath$	61.0675	0.0023	$61.1614 - 0.1801\imath$	61.1645

in Figs. 5 (b) and 5 (e), and for the near-resonance energy $E^{\rm res} \pm 0.1$ in Fig. 5. At $g = 0.001$ and $g = 0$, the resonance eigenfunctions, in contrast to the non-resonance ones, are localized in the potential well. At $g(E) > 0$, the degree of localization is less than at $g = 0$. Three metastable states correspond to three peaks of $g(E)$ in Fig. 3 (a), as shown in Fig. 6. So, at $g(E) > 0$, the absolute value of the imaginary part of energy is larger than at $g = 0$. We show in Table 1 the complex energy $E^M_{L,\nu}$ of metastable states and corresponding shape resonance energies $E^{\rm res} \approx \Re E^M_{L,\nu}$ of the elastic scattering at $L = 0$ and $g = 0$, and $g(E) > 0$. One can see that the imaginary parts of energy $\Im E^M_{L,\nu}$ increase with increasing value of the coupling constant $g(E) > 0$, that means decreasing a life time of metastable states.

5 Conclusions

The algorithm implemented in the MAPLE system for solving the scattering problem for a second-order ordinary differential equation of the OM with a complex-valued potential and regular BCs is presented. The complex-valued potential is a sum of the known real part of the potential, which includes the nuclear potential, the Coulomb potential, and the centrifugal potential, and the imaginary part of the potential, represented as a product of the unknown coupling constant parameter $g(E)$ depending on the collision energy E of a pair of ions and the derivative of the real part of the known nuclear potential with respect to the independent variable of the ODE.

The algorithm implements the solution of the inverse problem: the calculation of the unknown coupling constant $g(E)$ by means of secant method using as input the amplitudes of reflection $R(E)$ and transmission $T(E)$ of the model with IWBCs, calculated in advance using the standard MAPLE-implemented program KANTBP 4M [24]. The proposed algorithm is shown to provide one-to-one correspondence between the OM with a complex-valued potential and the model of IWBCs with a real-valued potential.

The efficiency of the proposed approach was illustrated by a numerical example of solving the scattering problem of a pair of heavy ions ^{16}O+^{144}Sm in the single-channel approximation of the coupled-channel method of the test desk given in Ref. [20]. The behavior of the coupling constant $g(E)$ is shown to possess a resonance structure that corresponds to the existence of metastable states, that manifest themselves as resonances in the elastic scattering in the region of energy, where the fusion cross section smoothly increases.

A generalization of the algorithm over the solution of the scattering problem in OM for a system of second-order ODEs using the updated KANTBP 4M and KANTBP 3.1 programs will allow a description of the experimental data on the cross section for deep sub-barrier fusion of a pair of heavy ions. We hope that the proposed algorithm will provide a wider application of the extended OM in a description of sub-barrier reactions of heavy ions.

Acknowledgments. The present research benefited from computational resources of the HybriLIT heterogeneous platform of the JINR. This publication has been supported by the Russian Foundation for Basic Research and Ministry of Education, Culture, Science and Sports of Mongolia (the grant 20-51-44001) and the Peoples' Friendship University of Russia (RUDN) Strategic Academic Leadership Program, project No.021934-0-000. This research is funded by Ho Chi Minh City University of Education Foundation for Science and Technology (grant No. CS.2021.19.47).

OCH acknowledges financial support from the Ministry of Education and Science of Mongolia (grant No. ShuG 2021/137). The work of PWW, CJL, and HMJ is supported by the National Key R&D Program of China (Contract No. 2022YFA1602302), the National Natural Science Foundation of China (Grants Nos. 12235020, 12275360, 12175314, 12175313, and U2167204), the Leading Innovation Project (Grant No. LC192209000701), and the project supported by the Directors Foundation of Department of Nuclear Physics, China Institute of Atomic Energy (12SZJJ-202305).

References

1. Feshbach, H., Porter, C.E., Weisskopf, V.F.: Model for nuclear reactions with neutrons. Phys. Rev. **96**, 448–464 (1954)
2. Buck, B., Stamp, A.P., Hodgson, P.E.: The excitation of collective states by inelastic scattering the extended optical model. Phil. Mag. J. Theor. Exp. Appl. Phys. **8**, 1805–1826 (1963)
3. Tamura, K.: Analyses of the scattering of nuclear particles by collective nuclei in terms of the coupled-channel calculation. Rev. Mod. Phys. **37**, 679–708 (1965)
4. Guenther, P.T., Havel, D.G., Smith, A.B.: Neutron scattering and the optical model near A = 208 and implications on the inelastic scattering cross section of uranium-238. Nucl. Sci. Eng. **65**, 174–180 (1978)
5. Mişicu, Ş, Esbensen, H.: Signature of shallow potentials in deep sub-barrier fusion reactions. Phys. Rev. C **75**, 034606 (2007)
6. Esbensen, H., Tang, X., Jiang, C.L.: Effects of mutual excitations in the fusion of carbon isotopes. Phys. Rev. C **84**, 064613 (2011)
7. Rawitscher, G.H.: Ingoing wave boundary condition analysis of alpha and deuteron elastic scattering cross sections. Nucl. Phys. **85**, 337–364 (1963)
8. Christensen, P.R., Switkowski, Z.E.: IWB analysis of scattering and fusion cross sections for the ^{12}C+^{12}C, ^{13}C+^{16}O and ^{16}O+^{16}O reactions for energies near and below the Coulomb barrier. Nucl. Phys. A **280**, 205–216 (1977)
9. Krappe, H.J., Shring, K.M., Nemes, M.C., Rossner, H.: On the interpretation of heavy-ion sub-barrier fusion data. Z. Phys. A. **314**, 23–31 (1983)
10. Hagino, K., Rowley, N., Kruppa, A.T.: A program for coupled-channel calculations with all order couplings for heavy-ion fusion reactions. Comput. Phys. Commun. **123**, 143–152 (1999)

11. Hagino, K., Takigawa, N.: Subbarrier fusion reactions and many-particle quantum tunneling. Prog. Theor. Phys. **128**, 1061–1106 (2012)
12. Back, B.B., Esbensen, H., Jiang, C.L., Rehm, K.E.: Recent developments in heavy-ion fusion reactions. Rev. Mod. Phys. **86**, 317–360 (2014)
13. Hagino, K., Ogata, K., Moro, A.M.: Coupled-channels calculations for nuclear reactions: from exotic nuclei to super heavy elements. Prog. Part. Nucl. Phys. **125**, 103951 (2022)
14. Samarin, V.V., Zagrebaev, V.I.: Channel coupling analysis of initial reaction stage in synthesis of super-heavy nuclei. Nucl. Phys. A **734**, E9–E12 (2004)
15. Zagrebaev, V.I., Samarin, V.V.: Near-barrier fusion of heavy nuclei: coupling of channels. Phys. Atom. Nucl. **67**, 1462–1477 (2004)
16. Zagrebaev, V.: Heavy Ion Reactions at Low Energies. In: Denikin, A., Karpov, A., Rowley, N. (eds.) Lecture Notes in Physics, vol. 963. Springer, Cham (2019). https://doi.org/10.1007/978-3-030-27217-3
17. Wen, P.W., et al.: Near-barrier heavy-ion fusion: role of boundary conditions in coupling of channels. Phys. Rev. C **101**, 014618 (2020)
18. Wen, P.W., Lin, C.J., Nazmitdinov, R.G., Vinitsky, S.I., Chuluunbaatar, O., Gusev, A.A., Nasirov, A.K., Jia, H.M., Góźdź, A.: Potential roots of the deep sub-barrier heavy-ion fusion hindrance phenomenon within the sudden approximation approach. Phys. Rev. C **103**, 054601 (2021)
19. Gusev, A.A., Chuluunbaatar, O., Vinitsky, S.I., Abrashkevich, A.G.: KANTBP 3.0: new version of a program for computing energy levels, reflection and transmission matrices, and corresponding wave functions in the coupled-channel adiabatic approach. Comput. Phys. Commun. **185**, 3341–3343 (2014)
20. Chuluunbaatar, O., Gusev, A.A., Vinitsky, S.I., Abrashkevich, A.G., Wen, P.W., Lin, C.J.: KANTBP 3.1: a program for computing energy levels, reflection and transmission matrices, and corresponding wave functions in the coupled-channel and adiabatic approaches. Comput. Phys. Commun. **278**, 108397 (2022)
21. Bohr, A., Mottelson, B.R.: Nuclear Structure. Single Particle Motion. V. I, W.A. Benjamin. New York, Amsterdam (1969)
22. Bohr, A., Mottelson, B.R.: Nuclear Structure. Nuclear Deformation. V. II, W.A. Benjamin. New York, Amsterdam (1974)
23. Karpov, A.V., et al.: NRV web knowledge base on low-energy nuclear physics. Nucl. Instr. Meth. Phys. Res. A **859**, 112–124 (2017)
24. Gusev, A.A., Hai, L.L., Chuluunbaatar, O., Vinitsky, S.I.: KANTBP 4M - program for solving boundary problems of the self-adjoint system of ordinary second order differential equations. http://wwwinfo.jinr.ru/programs/jinrlib/kantbp4m/indexe.html. Accessed 17 May 2023
25. https://www.maplesoft.com
26. Takigawa, N., Rumin, T., Ihara, N.: Coulomb interaction between spherical and deformed nuclei. Phys. Rev. C **61**, 044607 (2000)
27. Abramowitz, M., Stegun, I.A.: Handbook of Mathematical Functions. Dover, NY (1965)
28. Chuluunbaatar, O., et al.: Calculation of a hydrogen atom photoionization in a strong magnetic field by using the angular oblate spheroidal functions. J. Phys. A **40**, 11485–11524 (2007)
29. Gusev, A.A.: Symbolic-numeric solution of boundary-value problems for the Schrödinger equation using the finite element method: scattering problem and resonance states. In: Gerdt, V.P., Koepf, W., Seiler, W.M., Vorozhtsov, E.V. (eds.) CASC 2015. LNCS, vol. 9301, pp. 182–197. Springer, Cham (2015). https://doi.org/10.1007/978-3-319-24021-3_14